EXPLOSION SOURCE MODEL DEVELOPMENT IN SUPPORT OF SEISMIC MONITORING TECHNOLOGIES: APPLICATIONS OF NEW MODELS FOR SHOCK-INDUCED TENSILE FAILURE

Howard J. Patton

Los Alamos National Laboratory

Sponsored by the National Nuclear Security Administration

Award No. DE-AC52-06NA25396/LA08-FY08-029-NDD02

ABSTRACT

This paper reports on research activities for the second year of this project developing new explosion source models that include the effects of deep-seated, shock-induced tensile failure. Free surface interactions and the dynamics of shock-wave rebound are responsible for modes of tensile and shear failures leading to permanent deformations in a conical volume over the shot point. A vast majority of nuclear explosions worldwide were conducted under containment conditions that facilitated shock-induced tensile failure. The new model is a superposition of monopole + tectonic release + shock-induced tensile failure sources, the latter represented by a compensated-linear-vector dipole (CLVD) with vertical axis of symmetry. This model was used to explain why M_s for the North Korean test of 9 October 2006 is anomalously large for its m_b. The model also applies to the recent test of 25 May 2009.

Research this past year has been directed at three outstanding observations/problems that challenge our understanding of seismic wave generation by the explosion source. (1) *Anomalous surface waves for Balapan nuclear tests*. In the 70’s and 80’s, long-period surface waves from these tests were noted for large Love waves and Rayleigh waves with polarity reversals and significant time delays. Repeated attempts to model these observations with just tectonic release were not completely successful. New observations based on deglitched waveforms of the Borovoye archive (Baker et al., these Proceedings) bridge the frequency gap between long-period fundamental modes and higher modes making up the low frequency *Lg* spectrum. This additional bandwidth is needed to resolve source parameters of new models that include tensile failure as well as tectonic release. (2) *Source-related spectral modulations*. Modulations were first observed in the mid-90’s for *Lg* spectral ratios of Yucca Flats explosions. Since then they have been observed in *Pg* and *Lg* coda-wave spectra for Pahute and Yucca Flats explosions. The nearfield $Rg \rightarrow S$ scattering hypothesis explains spectral modulations as the result of interference between *Rg* waves excited by explosion and CLVD sources, causing modulation in the composite *Rg* wavefield which imprints its spectrum onto the scattered *P* and *S* waves making up regional phases. The strength of the CLVD relative to the monopole decreases with yield due to the increasing force of slapdown, which compacts weak materials and reduces static deformations associated with the CLVD. As such, the $Rg \rightarrow S$ scattering hypothesis predicts the existence of modulations in spectral ratios taken between shallow and deep explosions on Pahute Mesa. This prediction was validated by observations, which are being modelled for time histories of the CLVD source. (3) *Direct versus indirect generation of S waves*. A recent publication used plane-layered theory to argue against the importance of near-field scattering (indirect mechanisms) relative to direct generation by the CLVD source. Our studies show that the published results are in error due to (a) deficiencies of Earth models lacking low velocities near the free surface where *Rg* is excited and propagates, and (b) inadequacies of plane-layered theory for scattering estimates.

OBJECTIVE

The objective is to develop new analytical explosion source models based on seismic moment tensor theory for further improvement and advancement of regional seismic discrimination and yield estimation technologies. Such technologies rely heavily upon the source information contained in high-frequency shear (*S*) waves. The use of coda waves following regional *S* phases to estimate explosion yield is one example of an emerging technology offering great promise for improved nuclear monitoring. Unfortunately, an understanding of how explosions excite *S* waves is quite limited, and a widening gulf between theory and practice undermines our confidence to monitor broad areas at small yields. The new models will provide a physical basis for explosion-generated *S* waves and theoretical insights for advancing yield estimation and discrimination capabilities, thereby closing the gulf between theory and practice.

RESEARCH ACCOMPLISHED

This project builds upon spherical (monopole) explosion source models developed in the 1970's. An important aspect of those models is the theory relating seismic amplitudes of *P* waves directly to yield, depth of burial, and material properties of the source medium. Analytical relationships predicted by the theory draw upon empirical yield scaling behaviors of key model constructs, such as the elastic radius. Furthermore, the analytical nature of these models facilitated their use since they were easy to implement by researchers, and as such, they were widely applied to study the explosion source. Their application continues to this day, but with the recognition that a spherical point source is inadequate to explain *S*-wave generation.

Tensile failure is a source of asymmetry known to exist on most underground explosions, even those overburied for their yield. A kinematic description of shock-induced, deep-seated tensile failure is a compensated linear vector dipole CLVD with vertical axis of symmetry in extension. A CLVD can generate *S* waves directly and indirectly through efficient excitation of short-period surface waves (*Rg*) and subsequent scattering into *P* and *S* waves close to the source. My research introduces this source of asymmetry into spherical source models. The new model will require the development of scaling relationships like those for the elastic radius in the case of the spherical model, but for parameters of the tensile failure source, including centroid depth, source process time, and strength of the CLVD force system. A simple analytical form couched in seismic moment tensor theory will be adopted so that the model can be easily incorporated into researchers' preferred wave propagation codes for calculating synthetic seismograms.

This year's research is directed at three outstanding observations/problems that challenge our understanding of seismic wave generation by the explosion source: (1) anomalous observations of long-period surface waves excited by nuclear tests conducted at the Semipalatinsk Test Site (STS) in the 70's and 80's, including the generation of large Love waves and Rayleigh waves with polarity reversals and time delays; (2) spectral modulations starting with the coda of *Pg* waves and persisting down regional waveforms through arrival times for *Sn*, *Lg*, and *Lg* coda, as documented for Nevada Test Site (NTS) explosions in *Lg* spectral ratios and difference spectrograms (Gupta and Patton, 2008), and (3) the problem of regional *S* wave generation by two classes of mechanisms: (a) "direct" excitation involving trapped *pS* conversions in the crust and/or non-spherical sources of tensile and shear failure versus (b) "indirect" generation by near-source scattering of short-period Rayleigh waves (e.g., *Rg*→*S* scattering). Presented first herein is research concerning upper bound estimates of *Rg*→*S* scattering. This research has uncovered a possible physical explanation for *Pn*/*Lg* spectral ratios of STS explosions to turn upward at low frequencies (see Fisk, 2006). The discovery motivated the second research topic discussed where new source models are tested against fundamental- and higher-mode surface waves generated by STS explosions and recorded at Borovoye. I conclude with research investigating spectral modulations that were predicted on the basis of the *Rg*→*S* scattering hypothesis and confirmed by spectral ratio observations between shallow and deep explosions on Pahute Mesa.

Upper Bound Estimates on Rg→S scattering.

A recent paper by Stevens et al. (2009; hereafter referred to as SXB09) presents upper bound estimates of *Rg*→*Lg* scattering amplitudes using an energy conservation approach for plane-layered Earth models. Their results are based on calculations for two velocity models, one for low-velocity structures at NTS and the other for high-velocity structures at STS. For low-velocity structures, they conclude (1) *Rg*→*Lg* scattering is a viable mechanism only for *Rg* waves excited by the spherical source (e.g., monopole) below 0.3 Hz, (2) above 0.3 Hz, direct *Lg* from the spherical source will dominate, and (3) scattering of *Rg* excited by the CLVD source never dominates *Lg*. For high-velocity structures, direct *Lg* from the CLVD will dominate above 1 to 3 Hz, while at lower frequencies, *Rg*→*Lg* scattering amplitudes from the monopole exceed amplitudes of direct *Lg* and dominate over scattered *Rg* amplitudes from the CLVD.

A comments paper by Patton and Gupta (2009; hereafter referred to as PG09) points out (a) deficiencies in scattering estimates based on plane-layered velocity models and (b) bias in the results of SXB09 since their single-source spectra calculations do not account for wavefield interactions between monopole and CLVD sources and their velocity models are not representative of test site structures in the upper 2 km where *Rg* excitation and propagation take place. Contrary to conclusions (1) and (2) of SXB09, PG09 shows that upper bound estimates of *Rg* scattering exceed amplitudes of direct *Lg* for NTS velocity models with low-velocity surface layers (see Figure 1). Compared to *Rg* excitation by a spherical explosion source, CLVD excitation can be rich in high frequencies for shallow source depths (h) in low-velocity surface layers and an important factor in upper bound estimates of *Rg*→*Lg* scattering, in contradiction to conclusion (3). $M(\omega) \cdot A^0(\omega, h)$ in Figures 1 and 2 is the *Rg* excitation spectrum, where $M(\omega)$ is the Mueller-Murphy spectrum (Mueller and Murphy, 1971; MM71) and $A^0(\omega,h)$ is the reduced excitation spectrum (see Patton and Taylor, 2008) for the axisymmetric portion of the source involving only M_{zz} and $M_{xx} + M_{yy}$ elements of the moment tensor. The caluculation in Figure 1 is for a CLVD seismic moment M_{CLVD} equal to one half the monopole moment M_I (e.g., $K = 2$, see below).

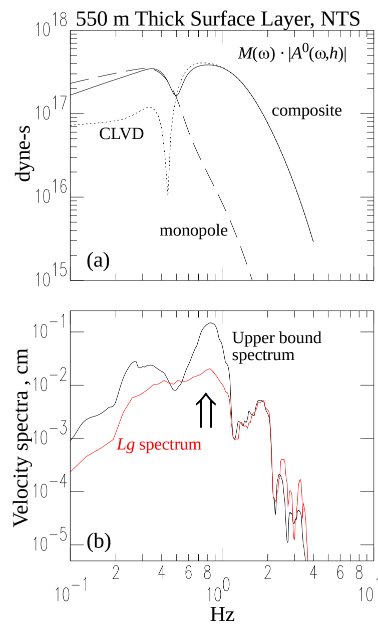

Figure 1. (a) *Rg* source excitation spectra for monopole, CLVD, and composite sources. (b) Composite upper bound *Rg* scattering spectrum and direct *Lg* spectrum for the SXB09 NTS structure with a 550 m thick low velocity surface layer. Both are multi-taper spectra. Arrow indicates the 0.6 to ~1.0+ Hz band where upper bound estimates of *Rg* scattering exceed the direct spectrum.

For high-velocity structures, SXB09 over-state their conclusion about the dominance of scattered waves excited by spherical sources since their calculations do not consider the effects of interactions between *Rg* wavefields radiated by the two sources. On the other hand, calculations in PG09 do so by taking the vector sum of wavefields excited by the monopole and CLVD sources (see Figures 1 and 2). Upper bound estimates based on vector-composite *Rg* spectra are better behaved than separate-source (monopole or CLVD) estimates of SXB09, and comparisons with direct *Lg* spectra are more meaningful since energy conservation should be based on composite *Rg* wavefields, not the wavefields excited by the separate sources. Furthermore, studies of the wavefield interactions at low-frequencies have led to a discovery that might explain interesting departures of *Pn*/*Lg* spectral ratio observations from model predictions (Fisk, 2006; 2007).

The *Rg* composite spectrum in Figure 2 is more peaked than either constituent spectrum and shows a pronounced roll-off in amplitude to low frequencies. This is a consequence of frequency-dependent cancellation between the monopole and CLVD wavefields. The roll-off is present in both upper bound and direct *Lg* spectra and increases as *K* increases (see next section). The source parameter *K* is proportional to the moment ratio, M_{CLVD} / M_I (see Patton and Taylor, 2008; also see equation in Figure 7 below). This roll-off feature is stable for a wide range of *K* values owing to two basic facts: (1) monopole and CLVD sources generate Rayleigh waves with opposite polarities for frequencies less than the CLVD excitation null and (2) the CLVD origin is delayed with respect to the monopole.

Below 1 Hz, *Rg* composite spectra in Figures 1a and 2a show that a low-frequency roll-off is expected to be more noticeable for explosions in hard rock media compared to NTS explosions, where the most obvious result of wavefield interactions is spectral modulation. Under the *Rg*→*S* scattering hypothesis and on the basis these predicted *Rg* composite spectra, spectral characteristics of farfield *S* waves below 1 Hz are expected to be different for STS and NTS explosions. Assuming the MM71 model for *Pn* waves and a flat spectrum at low frequencies, a roll-off in *Lg* spectra qualitatively agrees with the up-turn in STS *Pn/Lg* spectral ratio observations below 1 Hz documented in Fisk (2006). Likewise, modulation seen in the *Lg* spectra is consistent with *Pn/Lg* observations for NTS explosions in Fisk (2007).

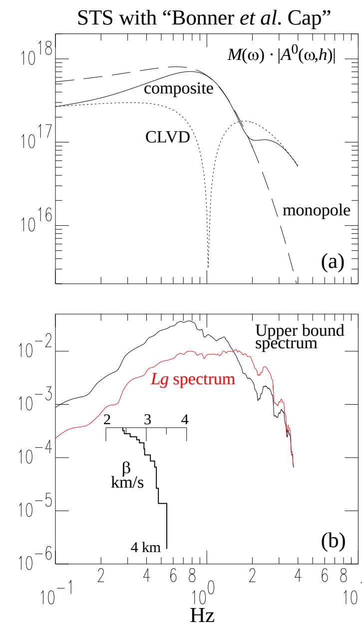

Figure 2. (a) *Rg* source excitation spectra for monopole, CLVD, and composite sources. Monopole and CLVD depths are 600 and 300 m, respectively. *K* = 2. (b) Composite upper bound *Rg* scattering spectrum and direct *Lg* spectrum for modified SXB09 Degelen structure with velocity gradient in the upper 1.5 km. Inset shows *S* profile for the top 4 km.

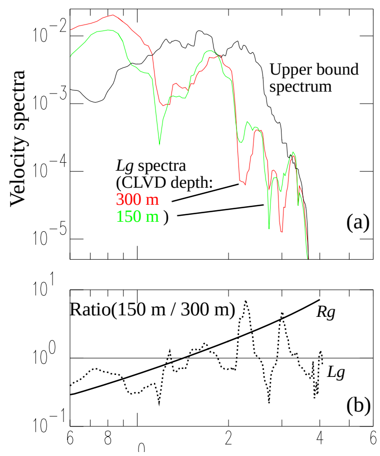

Figure 3. (a) Composite upper bound *Rg* scattering spectrum for a hybrid calculation where CLVD depth is 150 m. *Lg* spectra for 300 (red) and 150 m (green) CLVD source depths are shown for comparison. (b) Ratios of *Rg* source excitation spectra (solid line) and direct *Lg* spectra (dotted line) for composite sources, one with CLVD depth of 150 m and the other with CLVD of 300 m.

The importance of *Rg* scattering at high frequencies (> 3 Hz) ultimately depends on the relative excitation of *Rg* and *Lg* for very shallow sources. Explosions are far from being point sources of dilatation since significant deformations extend from below the shot point to the free surface. Depending on how the deformations are distributed in the column of material over the shot, a point-source CLVD model may have to be replaced by a finite source distributed over depth. We find that depth dependences of *Rg* and *Lg* excitation increase the relative importance of upper bound scattering estimates for very shallow sources. A “hybrid” calculation was run for the SXB09 NTS structure with a 550 m thick low velocity surface layer where the CLVD centroid depth is 150 m instead of 300 m as in Figure 1. In a hybrid calculation, scattering takes place in a different plane-layered structure than the structure in which excitation takes place (see PG09). The results for upper bound *Rg* scattering and direct *Lg* spectra are shown in Figure 3a. It can be seen that the upper bound spectrum is more robust for frequencies above 2 Hz compared to the 300 m case in Figure 1, while the average *Lg* spectral amplitudes remain unchanged. Further detail is provided in Figure 3b showing *Rg* and *Lg* ratios for composite sources where the only change is the CLVD source depth. Compared to the 300 m CLVD depth, the 150-m upper bound spectrum is richer in high frequencies simply because the *Rg* excitation is greater there. Meanwhile, the excitation of *Lg* waves has not changed significantly with respect to the 300 m case.

Tests of New Source Models Against Fundamental- and Higher-Mode Surface Wave Observations.

In the 70’s and 80’s, long-period excitation of surface waves by nuclear tests conducted at STS in central Asia were noted for anomalous behavior, including the generation of large Love waves and Rayleigh waves with polarity reversals and significant time delays (Rygg, 1979; Helle and Rygg, 1984). Repeated attempts to model the observations with tectonic release (Given and Mellman, 1986; Ekström and Richards, 1994) were not completely successful, although tectonic release models with reverse faulting explained observations the best (Harkrider, 1981; Day and Stevens, 1986; Day et al., 1987). New explosion source models for tensile failure represented by a CLVD have yet to be tested to see if they can explain the full suit of observations, including m_b-M_s scaling with respect to predictions of the Mueller-Murphy model. Due to broader frequency content and a fairly complete recording history of STS explosions, waveform data from the Borovoye archive (Baker et al., these Proceedings) offer an opportunity to re-evaluate old explosion source models and test new ones.

Some 50 Balapan explosions located in Northeast NE, Transition Zone TZ, and Southwest SW test areas (see Ringdal et al., 1992) are currently under study where epicenters and origin times are taken from Kim et al. (2001). For a map of these epicenters, see Figure 2 of Baker et al. (these Proceedings). Filtered vertical-component displacement traces of the TSG DS instrument system are plotted in Figure 4 along with epicentral distances to Borovoye (BRV), teleseismic m_b calculated by Blacknest seismologists (Ringdal et al., 1992), and a reference to the study of Ekström and Richards (1994; E&R94) for those events whose surface waves were analyzed for moment tensor descriptions. The traces are arranged in order of increasing distance from 679.7 to 696.1 km, a span of 16.4 km. Red and blue boxes demarcate the arrivals of fundamental- and higher-mode Rayleigh waves.

For large explosions in the study of Fisk (2006), signal-to-noise ratio (SNR) for *Pn* and *Lg* waves recorded at WMQ and MAK appears adequate for frequencies as low as ~0.2 Hz (see his Figure 11). *Pn/Lg* spectral ratios at low frequencies may be reliable for his large explosion groupings in Figures 14 - 17. The up-turn in Fisk's spectral ratio observations at low frequencies is qualitatively consistent with a roll-off in the spectrum of *Lg* waves if the low-frequency spectrum of *Pn* waves is flat as predicted by the MM71 model. A spectral analysis of higher modes making up *Lg* was conducted to examine the behavior of spectra at low frequencies.

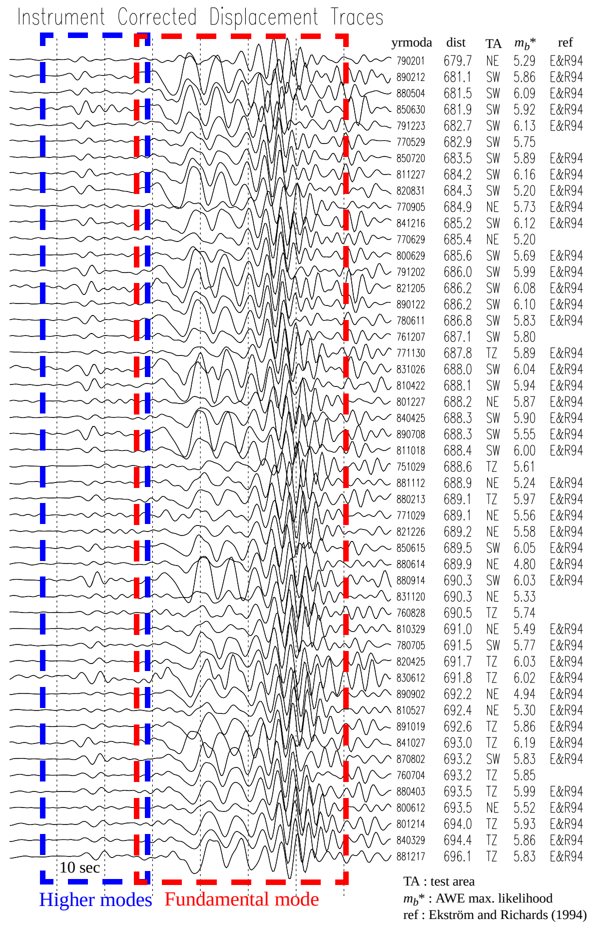

Figure 4. Profile of instrument-corrected, vertical-component displacement traces for the TSG DS instrument system ordered by increasing epicentral distance from the BRV. The frequency pass-band is 0.03 to 0.5 Hz.

Path-corrected *Lg* displacement spectra in Figure 5 were obtained by Fourier transforming BRV signals recorded on the DS instrument system for a time window corresponding to average apparent velocities of 3.77 and 3.21 km/s. For an average distance of 688 km, the corresponding window length is 32 s. A multi-taper algorithm was applied involving 512-point transforms and 7 tapers. Further details about SNR checks and corrections for attenuation may be found in Baker et al. (these Proceedings). Shown with the spectra are linear fits to the low frequency portion starting at 0.8 Hz. Low-frequency cut-offs of the fits were determined by SNR, but never went below 0.1 Hz. The legend on each spectrum provides test area, estimates of slope and one standard deviation, and the Blacknest m_b. An *R* in parentheses next to the test area indicates that Rayleigh waves are polarity reversed at BRV. This is the case for both NE shots. The shots are ordered by increasing slope moving left to right and top to bottom, and their magnitudes have been restricted to a range of just 0.3 magnitude units (mu) between 5.56 and 5.86. Because of this restricted range, I do not expect yield variations to have a significant impact on the shape of these spectra.

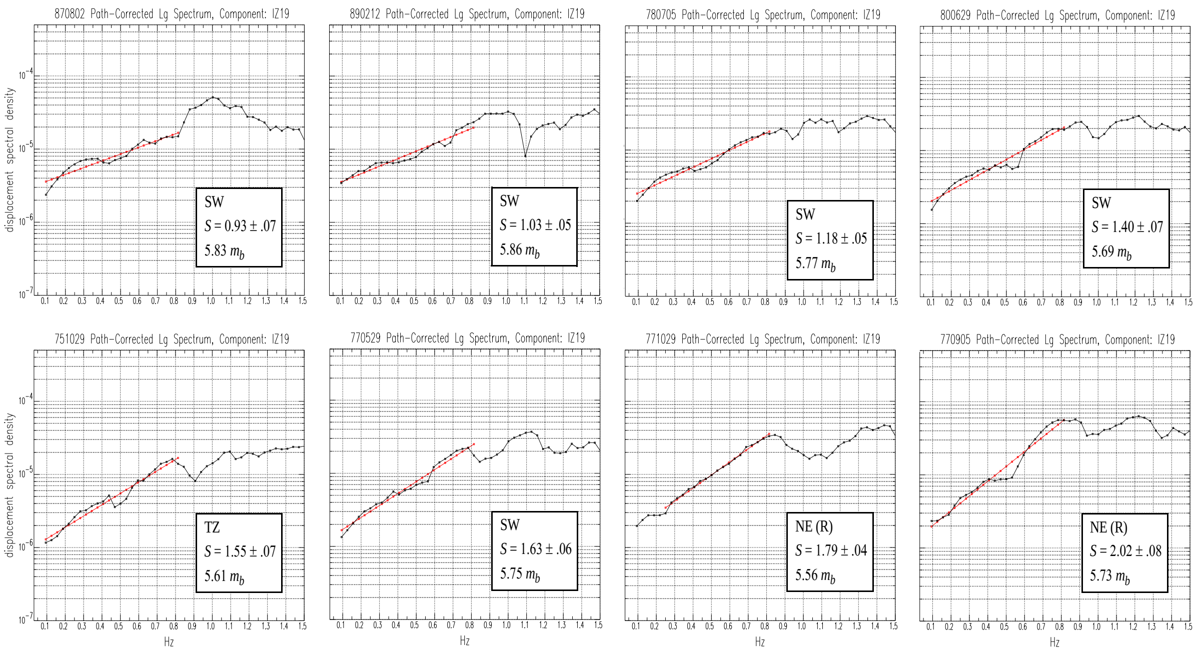

Figure 5. Path-corrected *Lg* displacement spectral densities for 8 Balapan shots recorded on the DS instrument system at BRV. The 6-digit code for year, month, day of the shot is printed in the title above each plot. Red lines are linear fits to the spectra for frequencies below 0.8 Hz. Slope estimates (*S*) and standard deviations are provided along with test area and m_b. The shots are restricted to a narrow range of source strengths based on m_b spanning only 0.3 mu.

Lg displacement spectra are not flat for frequencies below the corner frequency as expected based on the Mueller and Murphy model (Mueller and Murphy, 1971). Rather, the spectral amplitudes roll-off toward low frequency, consistent with the *Pn*/*Lg* observations of Fisk. Furthermore, shots with the highest slopes also show reversed polarity Rayleigh waves at BRV and negative U_1 values from the study of E&R94. These observation suggest a correlation between the low-frequency slope of *Lg* spectra and effects on longer-period fundamental-mode Rayleigh waves. Baker et al. (these Proceedings) explore this possibility in detail with their Figure 5 where the slope of the *Lg* spectrum is plotted against m_b–M_s; m_b is the Blacknest maximum-likelihood estimate and M_s is determined from BRV DS recordings using the Marshall and Basham method (Marshall and Basham, 1972). All M_s determinations but one are based on Rayleigh wave amplitudes in the 17 - 23 s period pass-band. As seen in Figure 5 of Baker et al., a correlation does exist between low-frequency *Lg* spectral slope and M_s corrected for source size using m_b. This finding is very interesting in the context of spectral ratio observations of Fisk (2006). While dismissed by Fisk as a result of noise contamination, the correlation suggests that upturn in *Pn*/*Lg* ratios is real, and is related to roll-off in *Lg* spectra at low frequencies.

Predictions from CLVD source models and the Rg→S scattering hypothesis. Here I will show that a low-frequency roll-off in *Lg* spectra for Balapan explosions can be modeled to first degree using a monopole + CLVD source model and invoking the *Rg*→*S* scattering hypothesis. According to this hypothesis, *Rg* waves radiated by the source are scattered into P and S waves in the nearfield, and the amplitude-frequency dependence of the incident wave is imprinted onto scattered waves. This basic tenet of seismic scattering traces it roots to early studies using coda waves to extract source spectra (e.g., Aki, 1969), and has been repeatedly proven true in many subsequent studies. Some scattered S waves are trapped in the crust and go on to become part of the far-field energy carried by *Lg* waves and its coda. SXB09 show that scattered *Rg* amplitudes far exceed the *Lg* amplitudes excited directly by explosion and CLVD sources in high velocity media for frequencies less than 1 Hz. GP09 concurs with their result, but point out that SXB09 overlooked *Rg* wavefield interactions between the two sources, which can significantly alter the amplitude-frequency dependence of radiated *Lg* waves as well as *Rg* before scattering occurs.

This fact is illustrated in Figure 6. Synthetic *Rg* and *Lg* excitation spectra (infinite Q) are plotted between 0.1 and 0.8 Hz for monopole + CLVD source models, where centroid depths are 600 and 300 m, respectively. A MM71 source function is assumed for both sources, and the origin of the CLVD is delayed by the time it takes a *P* wave to travel up to the free surface from the monopole and back down to the CLVD centroid depth. The only source parameter varied is *K*, the relative source strength of the CLVD. For each case, the spectrum has been offset by a factor of 2 from the previous one for plotting purposes. (Note the amplitude-frequency dependence is of interest, not the absolute amplitude; also relative amplitude between *Rg* and *Lg* is not preserved on these plots.) As with the observations in Figure 5, a linear fit of $\log_{10}$ amplitude versus frequency is applied to each spectrum, and the fits are shown in Figures 6a and b. Residuals from the fits to synthetic *Rg*, *Lg*, and observed *Lg* spectra have average 1-σ values of 0.094, 0.171, and 0.079, respectively, synthetic *Lg* spectra showing the highest departures from a straight-line approximation, while observed *Lg* spectra for 50 shots show the smallest, and synthetic *Rg* spectra slightly more. Indeed, the synthetic *Lg* spectrum for a pure monopole source (*K* = 1) is relatively flat out to 0.4 Hz and falls off rapidly at lower frequencies, and as do *Lg* spectra for other *K* values. Curvature in *Rg* spectra increases as *K* value increases.

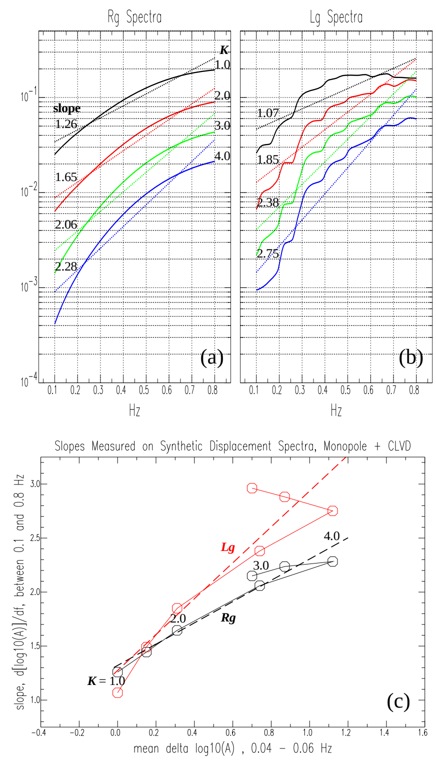

Figure 6. Excitation of *Rg* (a) and *Lg* waves (b) in the Degelen model of SXB09 modified for velocity gradient in the upper 1.5 km (see Fig. 2). Color coding is by *K* value, and linear fits for 0.1-0.8 Hz are shown with annotated slope values. (c) Slope values are plotted against $-M_s$ with respect to a pure monopole (*K* = 1) for synthetic Rayleigh wave spectral amplitudes averaged between 0.04-0.06 Hz. Dash lines are linear fits to 7 sample points; *K* values are annotated for several cases. *K* = 5 is the strongest CLVD source considered (M_{CLVD}/M_I = 1.14).

Cancellation of long-period Rayleigh waves radiated by an explosive monopole and a CLVD with vertical axis of symmetry in extension has been studied by Patton and Taylor (2008) for the effects on M_s, which make explosions discriminate better on m_b-M_s plots. For Rayleigh wave amplitudes measured near 20-s period, M_s decreases with increasing *K* until a value near 4 ($M_{CLVD}/M_I = 1$) in hard rock media, where Rayleigh waves reverse polarity and grow in amplitude for larger *K* values. Figure 6c shows the expected correlation between the predicted change in M_s (reduction then increase) and the slope measured on synthetic *Rg* and *Lg* spectra keeping yield fixed and varying *K*. *K* ranges from 1 to a maximum of 5 (1.0, 1.5, 2.0, 3.0, 4.0, 4.5, 5.0). As M_s decreases (e.g., $-M_s$ increases) with *K*, *Rg* and *Lg* slopes increase for 1<K<4. Above 4, *Lg* slopes continue to increase, while *Rg* slopes remain constant or decrease slowly. These results show that the scaling of slope values is faster for *Lg* waves than it is for *Rg* waves, as shown by the linear fits in Figure 6c to the results for 7 different *K* values. The scaling goes as 1.7 for *Lg* waves, while it is only 1.0 for *Rg*. A least squares estimate of scaling for observations in Figure 5b of Baker et al. is 0.7 ± 0.3 at the 2-σ level. This estimate is consistent with the preliminary results in Figure 6c for *Rg* waves. Future work will use more realistic source simulations including the effect of source depth and the inclusion of tectonic release. It should be noted however that BRV lies close to nodal plane for most tectonic solutions reported in E&R94, and thus we expect that this station is nearly optimal for studying axisymmetric effects predicted by just a monopole + CLVD model.

Spectral modulations predicted by the *Rg*→*S* scattering hypothesis and confirmation from NTS observations. Under the *Rg*→*S* scattering hypothesis, spectral characteristics of farfield *S* waves below ~1 Hz are expected to be different for STS and NTS explosions: in hard rock, *Lg* displays a pronounce low-frequency spectral roll-off, while for NTS media, the most noticeable feature is spectral modulation. Both features can be explained as the result of *Rg* wavefield interactions between monopole and CLVD sources (see Figures 1a and 2a above). Should the monopole dominate over the CLVD, effects of wavefield interactions are minimal, and the amplitude-frequency dependence of *Rg* waves will be controlled by the explosion source. Therefore, a prediction of the *Rg*→*S* scattering hypothesis is that low-frequency roll-off should lessen as $K \to 1$, as seen in Figure 6c, and spectral modulation should become muted to the point of vanishing.

An interesting result from Patton and Taylor (2008) was the inference that *K* decreases with yield for Pahute Mesa explosions ranging in size over 2 orders of magnitude. Measurements of *K* values based on moment tensor inversions support this finding (Figure 7). The reduction in *K* was interpreted to be a consequence of compaction, closing voids and less static deformation for the CLVD source as the force of slapdown increases with yield. Ignoring the effects of tectonic release, the largest Pahute Mesa shots look virtually isotropic, while *K* values for most explosions with $m_b < 5.75$ range between 1.4 and 2.5. The *Rg*→*S* scattering hypothesis predicts that modulation should be absent for large shots and yet present on smaller shots. This prediction can be tested by taking *Lg* spectral ratios between smaller and larger shots, similar to the approach of Patton and Taylor (1995), except in that study larger, normal-buried explosions were in the numerator and smaller overburied explosions in the denominator, just opposite to the way ratios are taken here.

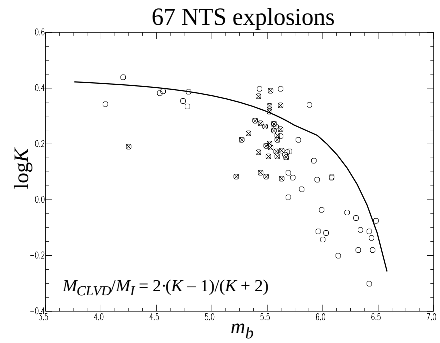

Figure 7. Comparison of inferred *K* (solid line) with measured *K* from moment tensor inversions. Pahute Mesa shots above the water table are plotted with circle-enclosed ×.

The explosion population was split into two groups on the basis of burial depth: 39 smaller events ranging between 540 and 690 m and 14 larger events between 820 and 1450 m. *Lg* displacement spectra were computed for a time window corresponding to apparent velocities of 4.0 and 2.8 km/s. Each $\log_{10}$ spectrum was made zero mean and a log-average was computed on a station by station basis for explosions in each group. Seven stations of the Livermore and Sandia regional NTS networks were used; Sandia stations DRW and TON were excluded because their epicentral distances are too short. Ratios between the average spectra for each group were taken. Figure 8 shows ratios for all 7 stations and the network average.

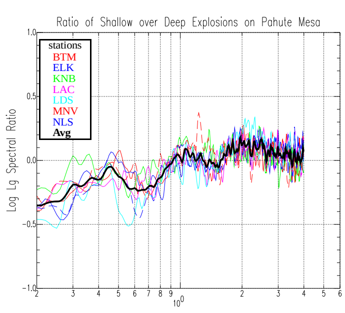

Figure 8. *Lg* spectral ratios by station and network (black line).

The conventional spectral ratio method employing an overburied (OB) explosion and nearby normal-depth explosions was applied to ALAMO, BACKBEACH, and NEBBIOLO with GALVESTON serving as the OB explosion. The *Lg* spectral ratios for these three shots are compared with the network results obtained from the shallow/deep explosion groupings in Figure 9. Modulations are observed in both types of spectral ratios, and there is good agreement between the two below 1 Hz, where the modulation shows a distinct null centered near 0.7 Hz. This is in contrast to Yucca Flats explosions, which show modulations and a null centered near 0.55 Hz (Patton and Taylor, 1995). Modulation persists above 1 Hz in the shallow/deep ratio, while the conventional ratios show too much scattered even for network averages using 6 Livermore and Sandia stations. Apparently, averaging many explosions in the shallow/depth ratio calculation has reduced the scatter enough to bring out modulation above 1 Hz. The high frequency trend in the shallow/deep ratio can be explained by averaging Mueller-Murphy source functions for explosions in each group and taking their ratio. This ratio is also plotted in Figure 9, where a MM71 source function for tuff was employed, and yields were computed from source depth using $h = 120 \cdot W^{1/3}$ in meters and W in kilotons. MM71 matches the general frequency trend of the shallow/deep ratio, but it cannot account for the modulations. In summary, a prediction of the $Rg \rightarrow S$ scattering hypothesis based on systematic reduction of K with yield is validated by shallow/deep *Lg* spectral ratio observations for explosions located on Pahute Mesa.

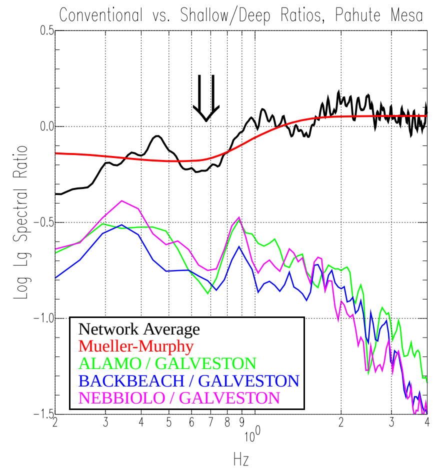

Figure 9. Comparison of *Lg* spectral ratios for conventional (normal-buried / overburied shot) method and network ratio for shallow / deep shots. Red curve is ratio of average MM71 source spectral ratio for shallow/deep groups

CONCLUSIONS AND RECOMMENDATIONS

In year 2 of this project, significant progress has been made developing explosion source models for the generation of *S* waves used heavily by discrimination and yield estimation technologies for regional, broad-area monitoring of nuclear tests at low yields. Three research topics that challenge our understanding of *S* waves generation were studied this year: (1) anomalous long-period surface wave excitation by STS explosions, first noted in the 70's and 80's, but never satisfactorily explained by tectonic release models alone; (2) the cause of spectral modulations observed in regional phases from NTS explosions and a prediction of the $Rg \rightarrow S$ scattering hypothesis; and (3) the relative importance of direct versus indirect (e.g., near-source scattering) mechanisms. These topics are very controversial among explosion seismologists. The role of tensile/shear failure represented by a CLVD source has been recognized and has gained greater acceptance in the community over past 5 years. Nevertheless, characterization of this source is in its infancy, and there is much exciting research ahead. I think there should be a concerted effort to develop an "effective" source time function for the CLVD that accounts for the fact that it is a distributed source and particle displacement time histories may vary significantly as a function of depth. For example, large impulsive particle motions may characterize shallow depths. On the other hand, motions at depth are smaller, yet probably couple better into the Earth and have larger permanent deformations and hence are the main source of CLVD moment.

ACKNOWLEDGEMENTS

The work reported herein has been conducted in part under a sub-contract with Lamont-Doherty Earth Observatory of Columbia University under the auspices of the Air Force Research Laboratory.

REFERENCES

Aki, K. (1969). Analysis of the seismic coda of local earthquakes as scattered waves, *J. Geophys. Res.* 74: 615–631.

Baker, D., W.-Y. Kim, H. J. Patton, G. E. Randall, and P. G. Richards (2009). Improvements to a major digital archive of seismic waveforms from nuclear explosions: The Borovoye seismogram archive, these Proceedings.

Day, S. M. and J. L. Stevens (1986). An explanation for apparent time delays in phase-reversed Rayleigh waves from underground nuclear explosions, *Geophys. Res. Lett.* 13: 1423–1425.

Day, S. M., J. T. Cherry, N. Rimer, and J. L. Stevens (1987). Nonlinear model of tectonic release from underground explosions, *Bull. Seismol. Soc. Am*. **77**: 996–1016.

Ekström, G. and P. G. Richards (1994). Empirical measurements of tectonic moment release in nuclear explosions from teleseismic surface waves and body waves, *Geophys. J. Int.* 117: 120–140.

Fisk, M. D. (2006). Source spectral modeling of regional *P/S* discriminants at nuclear test sites in China and the former Soviet Union, *Bull. Seismol. Soc. Am.* 96: 2348–2367.

Fisk, M. D. (2007). Corner frequency scaling of regional seismic phases for underground nuclear explosions at the Nevada Test Site, *Bull. Seismol. Soc. Am.* 97: 977–988.

Given, J. W. and G. R. Mellman (1986). Estimating explosion and tectonic release source parameters of underground nuclear explosions from Rayleigh and Love wave observations, Final report, Part I, AFGL-TR-86-0171(I), Air Force Geophysics Laboratory, Hanscom Air Force Base, MA, 70 pp.

Gupta, I. N. and H. J. Patton (2008). Difference spectrograms: A new method for studying S-wave generation from explosions, *Bull. Seismol. Soc. Am.* 98: 2460–2468.

Harkrider, D. G. (1981). Coupling near-source phenomena into surface wave generation, in *Identification of Seismic Sources--Earthquake or Underground Explosion, NATO Advanced Study Institute Series*, E. S. Huseby and S. Mykkeltveit, Editors, D. Reidel Publishing Co., Dordrecht, 277–326.

Helle, H. B. and E. Rygg (1986). Determination of tectonic release from surface waves generated by nuclear explosions in Eastern Kazakhstan, *Bull. Seismol. Soc. Am.* 74: 1883–1898.

Kim, W.-Y., P. G. Richards, V. Adushkin, and V. Ovtchinnikov (2001). Borovoye digital archive for underground nuclear tests during 1966-1996, Data report on the web at http://www.ldeo.columbia.edu/res/pi/Monitoring/Data/brv_exp_archive.html, Borovoye Archive for UNT (information product in PDF).

Marshall, P. D. and P. W. Basham (1972). Discrimination between earthquakes and underground explosions employing an improved M_s scale, *Geophys. J. R. Astr. Soc.* 28: 431–458.

Mueller, R. A. and J. R. Murphy (1971). Seismic characteristics of underground nuclear detonations Part I. Seismic spectrum scaling, *Bull. Seismol. Soc. Am.* 61: 1675–1692.

Patton, H. J. and S. R. Taylor (2008). Effects of shock-induced tensile failure on m_b-M_s discrimination: Contrasts between historic nuclear explosions and the North Korean test of 9 October 2006, *Geophys. Res. Lett.* 35: L14301.

Patton, H. J. and I. N. Gupta (2009). Comments on “An upper bound on *Rg* to *Lg* scattering using modal energy conservation” by Stevens, J. L., H. Xu, and G. E. Baker, *Bull. Seismol. Soc. Am.* 99: 906–913, 2009, submitted to *Bull. Seismol. Soc. Am*. April.

Ringdal, F., P. D. Marshall, and R. W. Alewine (1992). Seismic yield determination of Soviet underground nuclear explosions at the Shagan River test site, *Geophys. J. Int*. 109: 65–77.

Rygg, E. (1979). Anomalous surface waves from underground explosions, *Bull. Seismol. Soc. Am.* 69: 1995–2002.

Stevens, J. L., H. Xu, and G. E. Baker (2009). An upper bound on *Rg* to *Lg* scattering using modal energy conservation, *Bull. Seismol. Soc. Am.* 99: 906–913.